Guided Flash Lidar: A Laser Power Efficient Approach for Long-Range Lidar

Filip Taneski
Institute for Integrated Micro and Nano Systems
University of Edinbugh
Edinburgh, United Kingdom
ORCID: 0000-0002-3073-5855

Istvan Gyongy
Institute for Integrated Micro and Nano Systems
University of Edinbugh
Edinburgh, United Kingdom
ORCID: 0000-0003-3931-7972

Tarek Al Abbas
Ouster Automotive
Ouster, Inc.
Edinburgh, United Kingdom
ORCID: 0000-0002-5486-8791

Robert K. Henderson
Institute for Integrated Micro and Nano Systems
University of Edinbugh
Edinburgh, United Kingdom
ORCID: 0000-0002-0398-7520

***Abstract*—Solid-state flash lidar holds the potential for low-cost, scalable depth-sensing in self-driving vehicles. However, the conventional approach of storing and processing all photon arrivals becomes impractical over long (+200 m) distances, and alternative partial histogram solutions offer poor laser power efficiency. We propose a new approach, *guided* flash lidar, allowing other on-board sensors to narrow down the depth search space for a power-efficient flash lidar solution. We use a SPAD sensor containing 64-by-32 macropixels fabricated in a standard 40 nm CMOS process. Each macropixel is capable of timing and storing photon arrivals into 8 bins within an independently programmable time window to enable guiding. A pair of vision cameras guide each macropixel to a depth window of interest by providing stereo depth estimates. The system is shown to operate outdoors over a distance of 75 m while running at 3 fps. This is a 40-times laser cycle reduction over using a sliding partial histogram approach with the same sensor, and a 25-times data reduction over using a conventional approach. The capability for guided flash lidar to mitigate multipath reflections is also demonstrated by ranging through a glass door.**

Keywords—Lidar, time-of-flight, 3D vision, stereo depth.

I. Introduction

Combining lidar with other sensors such as cameras and radar, is widely considered to be the most safe and reliable design approach for self-driving vehicles [1, 2]. Automated driving safety frameworks such as those published by BMW and Volkswagen all follow a multi-sensory approach [3].

While traditional mechanical scanning lidar can achieve the necessary ranging performance, its high manufacturing cost, poor reliability, and frame rate limitations have made it less practical for use in commercial self-driving vehicles. On the other hand, solid-state *flash* lidar is a low-cost, scalable solution used in many indoor lidar applications such as smart phones and robotics. However, self-driving vehicles require lidar to perform over long distances (200 m) in outdoor environments. For flash lidar to meet these requirements, two critical challenges remain: high laser power consumption and large data volume. As illustrated in Fig. 1(a), to measure over longer distances requires the lidar sensor to count, store and process more photons over a wider temporal window. Novel

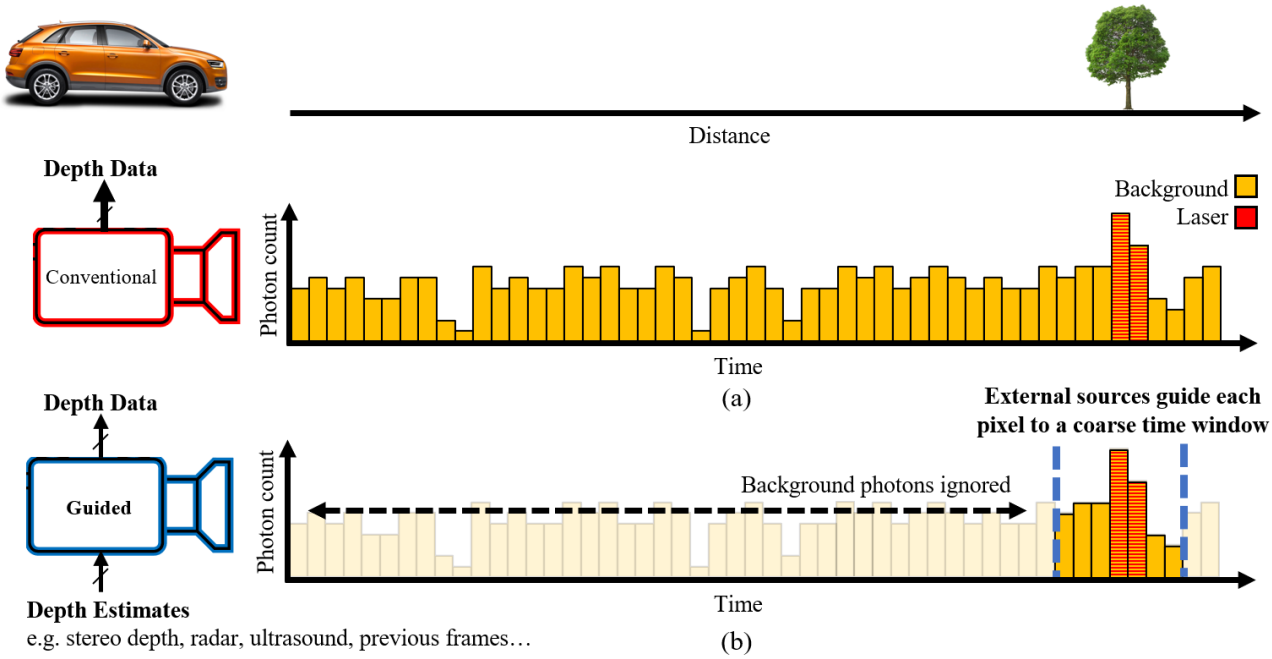

Fig. 1: Counting photon arrival events in (a) conventional flash lidar compared (b) to the proposed guided flash lidar approach.

"partial histogram" lidar sensors attempt to resolve this issue but do so at the cost of a severe laser power penalty [4].

This work showcases a new approach: *guided* flash lidar, which enables external sources to guide each pixel of the lidar to a coarse time window of interest (Fig. 1(b)). By utilizing data from other sensors on-board a self-driving vehicle to reduce the temporal search space, we propose that guided flash lidar can achieve the low power and data output required.

II. Related Work

Various alternatives over the conventional histogram approach (Fig. 1(a)) have been proposed to reduce the amount photon arrival data stored and processed on the lidar sensor. These *partial histogram* approaches can be grouped into two categories: *zooming* and *sliding*. Both are illustrated in Fig. 2.

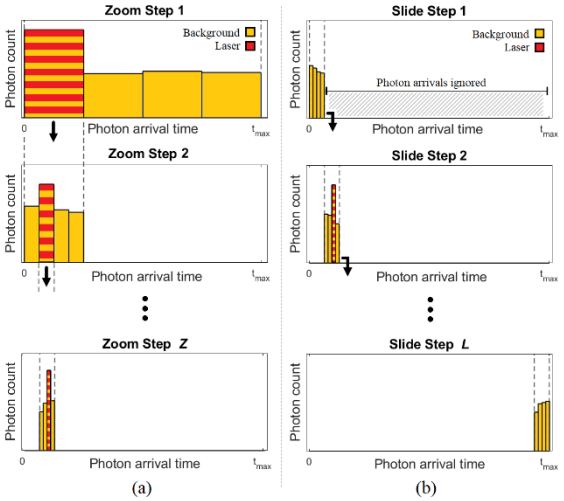

Fig. 2: Illustration of (a) zooming and (b) sliding histogram approaches.

In the zooming approach [5-8], the temporal histogram is initially spread across the full distance range. After multiple laser cycles, the peak (signal) bin is identified, and the histogram is zoomed in to a new, narrower time window. Multiple zoom steps can be performed until the required precision is achieved. In contrast, the sliding approach [9], spreads the histogram across only a subset of the sensing range and gradually slides the time window to cover the full range.

A major disadvantage of all partial histogram approaches is the severe laser cycle penalty they incur. In zooming, the wider time window used in earlier zooming steps leads to a high background photon count in the signal bin. As a result, many laser cycles are required to identify the peak bin. In the case of sliding, most laser pulses returning from the target fall outside of the window being observed at any one time. As a result, every L sliding steps used leads to an L-times increase in laser cycles and power. An in-depth review and analysis of partial histogram approaches is given in [4].

While partial histogram approaches may be sufficient for indoor applications, a more power-efficient solution is required for operating over long distances and under high ambient conditions. Although lidar is an effective solution for measuring depth to within centimeter precision, other sensors on-board a vehicle are also capable of providing range data. These include cameras, ultrasound, radar, and GPS/mapping data. A guided approach can use this data to reduce the depth search space, instead of the inefficient partial histogram approach of relying exclusively on the lidar to do so.

III. Guided Lidar System

A. Guided Lidar Sensor

The sensor used to demonstrate this approach (Fig. 3) was implemented in a standard 40 nm CMOS process and contains 64×32 macro pixels. Each macropixel is comprised of 4×4 SPADs alongside processing for timing and storing photon events into 8×12-bit time bins. The primary function of this sensor, originally presented in [10], allows each pixel to independently scan through time windows until a target (peak) is detected, at which point scanning stops and the peak is tracked as it moves into adjacent time windows. In this work, the sensor is reengineered to allow the time window of every pixel to be continuously and independently programmed.

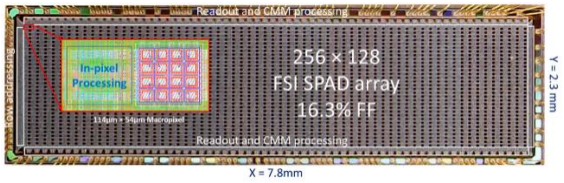

Fig. 3: Micrograph of the sensor used to demonstrate guided flash lidar

B. Depth Estimates Source: Stereo Depth

The presented implementation uses a pair of imaging cameras to provide stereo depth estimates for guiding the lidar sensor. This utilizes the resulting shift in pixel value (termed disparity) of matched points between each camera image to estimate distance. Distance z is given as a function of disparity d, camera baseline B and focal length f by:

$$z = \frac{fB}{d} \tag{1}$$

Relying on pixel disparity results in discrete depth estimates which limits depth resolution. This resulting depth accuracy Δd is given by:

$$\frac{\Delta z}{\Delta d} = \frac{fB}{d^2} \quad \Rightarrow \quad |\Delta z| = \frac{z^2 \Delta d}{fB} \tag{2}$$

Through interpolation, sub-pixel disparity Δd as low as 0.1 pixels is achievable. In practice, accuracy is limited by the performance of the adopted disparity matching algorithm. For the purpose of demonstrating guided flash lidar, the well-established semi-global matching (SGM) algorithm [11] is used as a convenient and time-efficient solution.

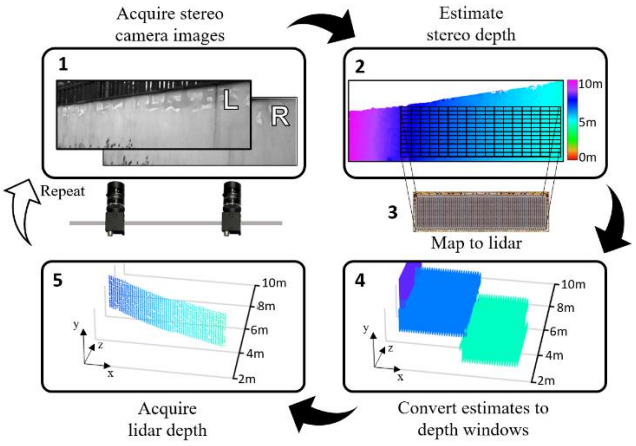

Fig. 4: Process flow of guided flash lidar using stereo depth estimates.

C. Process Flow

The processes involved in guiding the flash lidar sensor are shown in Fig. 4. The process begins by acquiring images from the stereo cameras, followed by solving the disparity between images to estimate depth. By prior calibration of the cameras and lidar using checkerboard images, the intrinsic parameters of all cameras and their pose with respect to each other is determined. This allows accurate mapping of the stereo depth image to each pixel on the lidar sensor. Finally, the depth estimate assigned to each pixel is converted to a time (depth) window and the guided sensor only counts returning photons within its assigned depth window.

D. Setup

The guided lidar setup, running off an Intel Core i7 8th generation laptop, is show in Fig. 5. It consists of:

- the lidar sensor mounted with 25 mm lens and 940 nm bandpass filter (10 nm full width half maximum)
- a 940nm laser module running at 80 kHz
- 2 × FLIR Blackfly BFS-U3-16S2M-CS cameras with 12 mm lenses, mounted on a meter-length rail
- a Bosch GLM250VF rangefinder for ground truth

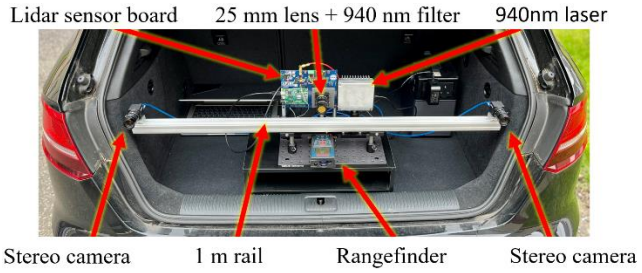

Fig. 5: Guided lidar setup

The sensor is configured to use 3 m wide depth windows (8×0.375 m bins) with a 1.125 m overlap. A maximum of 128 windows provides 240 m of unambiguous range. Wider depth windows (and bins) would give a greater safety margin for the guiding depth estimates at the cost of lidar accuracy.

IV. Guided Lidar Performance

A. Dynamic Outdoor Scene

Fig. shows a sample frame captured by the guided lidar system operating outdoors (15 klux) at 3 fps. It shows the stereo cameras creating depth estimates which are converted into coarse depth windows across objects in the scene such as the van. Every pixel then resolves any signal peak found in its allotted window to produce an accurate depth map. Further frames from the scene are given in Fig. 7 showing a sample pixel guided to follow the van as it drives away as far out as 75 m. A sliding partial histogram approach would otherwise require stepping through each of the 40+ depth windows, resulting in a 40 × laser cycle and power increase. Alternatively, a conventional histogram approach would require storing 200 bins per macropixel as opposed to only 8.

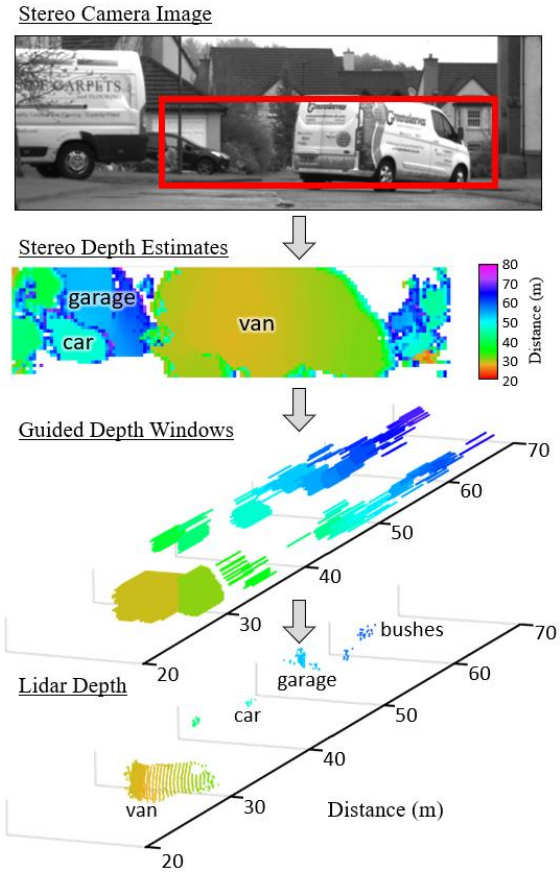

Fig. 6: One frame from the guided lidar system broken down into its component parts. Here the system is operating outdoors at 3 fps.

The processing time for each step of the system within a single frame is provided in Fig. 8, showing the lidar exposure period to be dominate most of the frame time. In short range indoor settings, runtimes exceeding 5 fps are achievable.

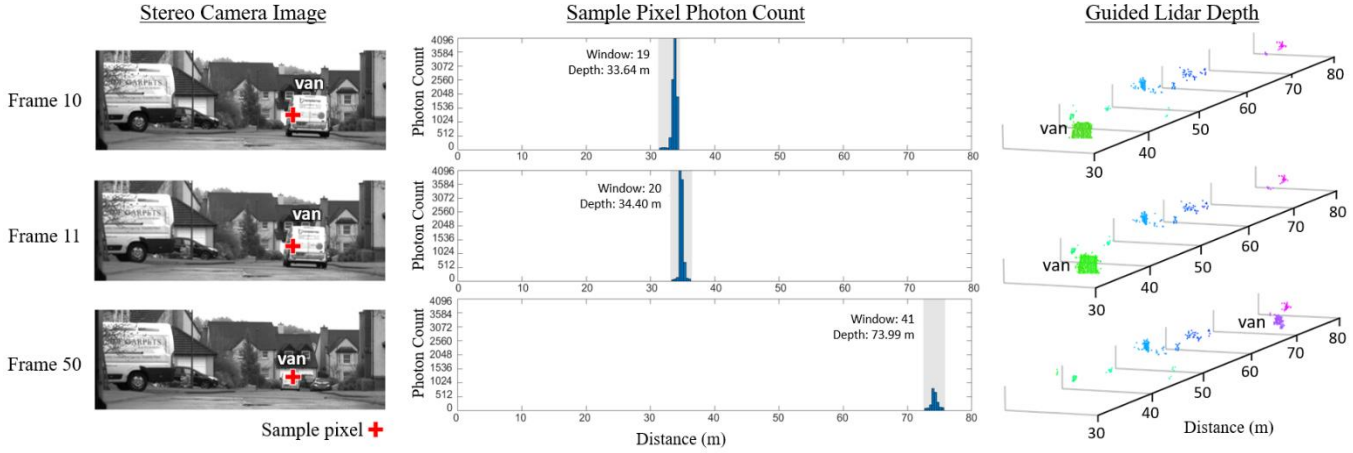

Fig. 7: Three further frames from the scene in Fig. 6 showing the time window of a sample pixel guided to track the moving van.

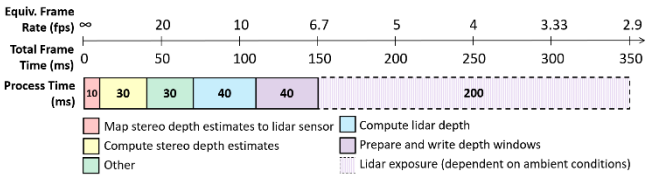

Fig. 8: Processing time of each step in one frame of the guided lidar system.

B. *Outdoor Accuracy*

The same setup running at 3 fps was used to perform a distance sweep up to 50 m under a higher ambient light condition of 72 klux. The combined precision and accuracy were evaluated by ranging a human target at 81 different points (3×3 pixels over 9 frames). The results are shown in Fig. 9, demonstrating that while the stereo depth accuracy deteriorates with distance, the guided lidar system maintains a root-mean-squared error of less than 20 cm.

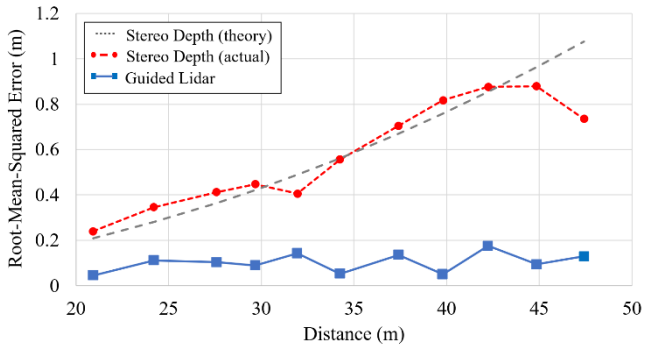

Fig. 9: Outdoor (72 klux) ranging performance operating at 3 fps. Theoretical stereo depth accuracy as given by (2) assumes sub-pixel disparity of 0.25.

C. *Guiding Through Glass*

Another benefit of guided flash lidar is mitigating multipath reflections. These can lead to ranging artefacts in the face of transparent surfaces or glare [12]. Fig. 10 shows the system is guided to the human figure beyond the glass door which is otherwise obscured if only the first peak is captured i.e. using zooming partial histogram approaches.

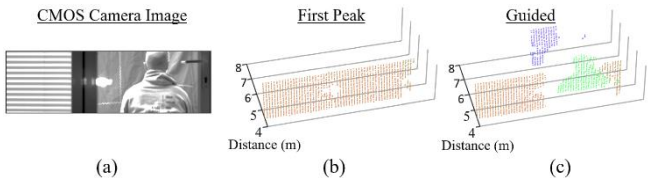

Fig. 10: (a) A human behind a glass screen is (b) obscured when using the first detected laser peak (c) revealed using guided lidar.

V. Summary

The first ever guided flash lidar system has been demonstrated. The presented system is capable of operating at 3 fps under high ambient daylight conditions of 72 klux. Outdoor ranging up to 75 m is demonstrated, with each macropixel being guided to one of over 40 separate depth windows. This results in a 40× reduction in laser cycles (and laser power) over a sliding partial histogram approach. An equivalent performance using a conventional histogram approach would require the sensor to accommodate 25× more bins of storage per pixel. Guided flash lidar is also shown to mitigate against multipath reflections, successfully ranging though a glass door.

To improve performance, future design iterations could explore alternative guiding sources and parallelizing tasks within a frame. Combining a guided lidar approach with the increased sensitivity of state-of-the-art SPAD processes [13, 14] would greatly reduce the required exposure time to range over longer distance and/or using shorter exposure periods.

Acknowledgment

The authors sincerely thank Ouster, Inc. for funding this research and Prof. Robert Fisher for guidance on stereo depth.

References

[1] S. Rangwala, "Automotive LiDAR Has Arrived." [Online]. Available: https://www.forbes.com/sites/sabbirrangwala/2022/05/23/automotive-lidar-has-arrived/?sh=1f164cf013de

[2] Z. Wang, Y. Wu, and Q. Niu, "Multi-Sensor Fusion in Automated Driving: A Survey," *IEEE Access,* vol. 8, pp. 2847-2868, 2020, doi: 10.1109/ACCESS.2019.2962554.

[3] Aptiv *et al.*, "Safety First For Automated Driving [White Paper]," 2019. [Online]. Available: https://group.mercedes-benz.com/documents/innovation/other/safety-first-for-automated-driving.pdf

[4] F. Taneski, T. A. Abbas, and R. K. Henderson, "Laser Power Efficiency of Partial Histogram Direct Time-of-Flight LiDAR Sensors," *Journal of Lightwave Technology,* vol. 40, no. 17, pp. 5884-5893, 2022, doi: 10.1109/JLT.2022.3187293.

[5] C. Zhang, S. Lindner, I. M. Antolović, J. M. Pavia, M. Wolf, and E. Charbon, "A 30-frames/s, 252 x 144 SPAD Flash LiDAR With 1728 Dual-Clock 48.8-ps TDCs, and Pixel-Wise Integrated Histogramming," *IEEE Journal of Solid-State Circuits,* vol. 54, no. 4, pp. 1137-1151, 2019, doi: 10.1109/JSSC.2018.2883720.

[6] B. Kim *et al.*, "7.2 A 48×40 13.5mm Depth Resolution Flash LiDAR Sensor with In-Pixel Zoom Histogramming Time-to-Digital Converter," in *2021 IEEE International Solid- State Circuits Conference (ISSCC)*, 13-22 Feb. 2021 2021, vol. 64, pp. 108-110, doi: 10.1109/ISSCC42613.2021.9366022.

[7] C. Zhang *et al.*, "A 240 x 160 3D Stacked SPAD dToF Image Sensor with Rolling Shutter and In Pixel Histogram for Mobile Devices," *IEEE Open Journal of the Solid-State Circuits Society,* pp. 1-1, 2021, doi: 10.1109/OJSSCS.2021.3118332.

[8] S. Park *et al.*, "5.3 An 80×60 Flash LiDAR Sensor with In-Pixel Histogramming TDC Based on Quaternary Search and Time-Gated Δ-Intensity Phase Detection for 45m Detectable Range and Background Light Cancellation," in *2022 IEEE International Solid- State Circuits Conference (ISSCC)*, 2022.

[9] D. Stoppa *et al.*, "A Reconfigurable QVGA/Q3VGA Direct Time-of-Flight 3D Imaging System with On-chip Depth-map Computation in 45/40nm 3D-stacked BSI SPAD CMOS," in *International Image Sensor Workshop 2021*, 2021.

[10] I. Gyongy *et al.*, "A Direct Time-of-flight Image Sensor with in-pixel Surface Detection and Dynamic Vision," *IEEE Journal of Selected Topics in Quantum Electronics,* pp. 1-12, 2023, doi: 10.1109/JSTQE.2023.3238520.

[11] H. Hirschmuller, "Stereo Processing by Semiglobal Matching and Mutual Information," *IEEE Transactions on Pattern Analysis and Machine Intelligence,* vol. 30, no. 2, pp. 328-341, 2008, doi: 10.1109/TPAMI.2007.1166.

[12] I. Gyongy, N. A. Dutton, and R. K. Henderson, "Direct Time-of-Flight Single-Photon Imaging," *IEEE Transactions on Electron Devices,* pp. 1-12, 2022, doi: 10.1109/TED.2021.3131430.

[13] O. Kumagai *et al.*, "7.3 A 189×600 Back-Illuminated Stacked SPAD Direct Time-of-Flight Depth Sensor for Automotive LiDAR Systems," in *2021 IEEE International Solid- State Circuits Conference (ISSCC)*, 13-22 Feb. 2021 2021, vol. 64, pp. 110-112, doi: 10.1109/ISSCC42613.2021.9365961.

[14] K. Morimoto *et al.*, "3.2 Megapixel 3D-Stacked Charge Focusing SPAD for Low-Light Imaging and Depth Sensing," in *2021 IEEE International Electron Devices Meeting (IEDM)*, 11-16 Dec. 2021 2021, pp. 20.2.1-20.2.4, doi: 10.1109/IEDM19574.2021.9720605.